


ARTICLE

Open Access



An automated fluorescent immunoassay for on-site screening of AFM1 in raw milk at the ppt level

Jiaqian Kou¹, Leina Dou¹, Ghulam Mujtaba Mari^{1,3}, Weilin Wu¹, Yingjie Zhang¹, Peipei Li¹, Xiaonan Wang¹, Suxia Zhang¹, Kai Wen¹, Yiping Chen^{2*} and Wenbo Yu^{1*} 

Abstract

In the dairy industry, the quality of raw milk as it is collected from dairy farmers must be strictly ensured. Therefore, when on-site screening of typical carcinogens in raw milk, this technology must simultaneously be convenient to operate and highly sensitive. Here, an automated and fluorescent immunoassay system for screening trace amounts of aflatoxin M1 (AFM1) in raw milk was developed. The whole immunoassay procedure can be processed in a true “sample-to-results” paradigm, avoiding the tedious manual operation of the traditional indirect competitive enzyme-linked immunosorbent assay (ic-ELISA) method. In addition, we designed an integrated fluorescent spectrometer that can quantitatively measure fluorescent signals with high sensitivity. The automated and fluorescent immunoassay system can screen AFM1 in raw milk samples with an ultra low limit of detection (4.7 pg/mL in raw milk). The half maximal inhibitory concentration (IC₅₀) was 8.3 pg/mL, which is approximately 4-fold lower than that of traditional ic-ELISA. When the system was applied to screen actual raw milk samples, the recovery rates ranged from 79.4% to 104.6%, with a coefficient of variation ranging from 8.9% to 15.2%. Overall, we believe that the automated and fluorescent immunoassay system can provide a one-stop solution that is user-friendly and highly sensitive for screening trace AFM1 contaminants in raw milk.

Keywords AFM1, An automated immunoassay, An integrated fluorescent detector, Raw milk, Contaminants screening

Introduction

Aflatoxins (AFs) are a family of extremely toxic secondary metabolites that are produced by *Aspergillus flavus* and *Aspergillus parasiticus* [1]. Among the approximately 20 derivatives of AFs, AFM1 is the hydroxylated derivative of aflatoxin B1 (AFB1) and can be found in milk or other food items. When humans ingest food contaminated by AFM1, the toxin may cause carcinogenicity, mutagenesis, teratogenesis, genotoxicity, and immunosuppression [2]. Considering its acute toxicity to humans [3], the International Agency for Research on Cancer (IARC) of the World Health Organization (WHO) has classified AFM1 as a group 1 carcinogen [4, 5]. In addition, the safety of milk consumption has been largely focused

*Correspondence:

Yiping Chen
chenyiping@mail.hzau.edu.cn
Wenbo Yu
yuwenbo@cau.edu.cn

¹ National Key Laboratory of Veterinary Public Health and Safety, Beijing Key Laboratory of Detection Technology for Animal-Derived Food Safety and Beijing Laboratory for Food Quality and Safety, College of Veterinary Medicine, China Agricultural University, Beijing 100193, People's Republic of China

² Key Laboratory of Environment Correlative Dietology, Ministry of Education, College of Food Science and Technology, Huazhong Agricultural University, Wuhan 430070, People's Republic of China

³ Department of Veterinary Pharmacology and Toxicology, Faculty of Bio-Sciences, Shaheed Benazir Bhutto University of Veterinary and Animal Sciences, Sakrand 67210, Pakistan



© The Author(s) 2024. **Open Access** This article is licensed under a Creative Commons Attribution 4.0 International License, which permits use, sharing, adaptation, distribution and reproduction in any medium or format, as long as you give appropriate credit to the original author(s) and the source, provide a link to the Creative Commons licence, and indicate if changes were made. The images or other third party material in this article are included in the article's Creative Commons licence, unless indicated otherwise in a credit line to the material. If material is not included in the article's Creative Commons licence and your intended use is not permitted by statutory regulation or exceeds the permitted use, you will need to obtain permission directly from the copyright holder. To view a copy of this licence, visit <http://creativecommons.org/licenses/by/4.0/>.

on worldwide. To protect consumers from the danger of AFM1, the maximum levels have been set in food of animal origin. For milk, China [6, 7], the United States [8, 9], and the European Commission [10] set the maximum levels at 0.5, 0.5, and 0.05 ng mL⁻¹, respectively. Consequently, in dairy enterprises, the quality of raw milk from its source must be strictly ensured when the milk is collected from dairy farmers. The most effective way to ensure the quality of raw milk is on-site screening of AFM1 at the source, and to perform this, the detection method must exhibit several properties, including being convenient to operate, highly sensitive, and inexpensive.

To detect AFM1, traditional analytical techniques, including chromatography and spectroscopy, exhibit several advantages, including high sensitivity and accuracy [11, 12]. However, these methods are time-consuming, require expensive and bulky instruments, and highly trained personnel [13, 14]. Hence, these methods are inappropriate for low-cost, on-site, and rapid screening. Immunoassays, as an efficient biological analysis method, have become the “gold standard” for rapidly screening contaminants in milk. Enzyme-linked immunosorbent assay (ELISA) [15] and lateral flow immunoassay (LFIA) [16] are commonly used in milk safety analyses. Among them, the 96-well microplate-based ELISA provides relatively high throughput, sensitivity, and semiquantitative detection. However, the process of manually operating traditional ELISA is complicated, and the sensitivity of ELISA is also affected by the characteristics of heterogeneous immune reactions that occur. LFIA is inexpensive, involves a simple operation and visual detection by using gold colloidal or other nanoparticles [17], and has become one of the most commercially viable analytical methods for screening contaminants. However, LFIA is limited by its low sensitivity and inability to detect trace amounts of contaminants, which requires an extremely sensitive method for detection. Therefore, it is urgent to upgrade the current immunoassays for the rapid detection of AFM1.

Immuno magnetic beads (MBs) have attracted strong interest in recent years due to their large specific surface area and magnetic separation properties [18]. Thus, MBs are often used as carriers of homogeneous immune reactions [19, 20] and separation tools [21–23] in the modern diagnostic field. In previous studies, our laboratory developed novel immunoassays using immuno MBs, which can significantly improve the detection performance of medical diagnosis [19] and contaminant detection in food items [22]. In addition, in the study of immunoassay signaling strategies, fluorescent-based immunoassays have been greatly developed in recent years [24]. Several novel fluorescent labeling [25] and sensing [26–28] methods have been established to improve the sensitivity of

immunoassays. However, for the detection of fluorescent signals, sophisticated instruments (including excitation light sources and detectors) are usually needed, and these instruments are not suitable for on-site screening due to their large size and high cost. Therefore, with the purpose of screening trace levels of AFM1 in milk samples, developing new approaches that are convenient to operate [29–31] and offer inexpensive signal quantification [32, 33] is an urgent task.

In this study, an automated and fluorescent immunoassay system was established to screen trace amounts of AFM1 in raw milk. This system utilizes immuno MBs as the immune reaction carriers for homogeneous immunoassays, which greatly improves the efficiency of antigen and antibody recognition. Combined with an automated immunoassay device, a “sample-to-result” screening paradigm was developed. In addition, trace amounts of AFM1 in raw milk were detected with high sensitivity through an enzyme-catalyzed strategy, involving a fluorescent “turn-on” signal and an exquisite and low-cost integrated fluorescent spectrometer. The automated and fluorescent immunoassay system has several advantages, as it is convenient to operate and achieves detection at the ppt level, which can sufficiently meet the maximum levels placed by various countries for AFM1 in raw milk. We believe that the automated and fluorescent immunoassay system will have great potential for application in the on-site screening of typical trace carcinogen and other analytes in milk.

Results and discussion

Characterization of the mAbs

Because AFM1 is a small molecule, it must be associated with a carrier protein to induce a particular immunological response. By introducing CMO, the hapten AFM1-CMO can be attached to the carrier protein KLH or BSA by the carboxymethyl hydroxylamine method. Matrix-assisted laser desorption time-of-flight mass spectrometry (MALDI-TOLF-MS) was used to determine the hapten-to-protein molar ratios. As shown in Fig. S1, after the hapten was conjugated with carrier protein, a peak shift was observed, and the molecular weight of hapten-to-BSA was 67,152.5 Da, which was higher than the molecular weight of BSA (66430 Da), indicating that the conjugation of AFM1-CMO with BSA was successful, and the ratio of hapten-to-BSA was 2.2. After mouse immunization, cell fusion and limited dilution method screening were performed, four hybridoma cell lines, namely, 10F8, 19E2, 13D4, and 3F8 were obtained, and these cell lines secreted antibodies with high affinity and exhibited AFM1 inhibition. According to the results of class and subclass determinations by antibody isotyping tests, the heavy chains of all mAbs were identified as

IgG1, whereas the light chains of all mAbs were determined to be of the Lambda type (Fig. S2).

To find the optimal combination of coating antigen and antibody, we examined three antigens and four mAbs by using ic-ELISA to measure sensitivity. The OD_{max} (OD value of the negative control), IC_{50} (half maximal inhibitory concentration), and OD_{max}/IC_{50} values of ic-ELISA for AFM1 from different combinations were shown in Fig. S3. The OD_{max}/IC_{50} ratio was used as the evaluation criterion of the ic-ELISA, in which a higher ratio indicated that the ic-ELISA had a higher sensitivity. As shown in Fig. S3C, the highest ratio of OD_{max}/IC_{50} was generated by the combination of AFM1-BSA and mAb 10F8. Therefore, the coating antigen AFM1-BSA and mAb 10F8 were used in subsequent studies (Table S1). Apart from coating antigen and antibody combination, other important immunoassay conditions, including ionic strength of dilution buffer (0 to 1160 mM NaCl content) and pH value (4.0 to 10.0 for PBS), were optimized. The OD_{max}/IC_{50} values at different ionic strengths and pH levels are shown in Fig. 1. Figure 1A shows that the ratio of OD_{max}/IC_{50} was highest at an ionic strength of 290 mM, which compared with that without ionic strength, was considerably improved. Figure 1B suggests that the neutral conditions were the optimal pH in the range of 4.0–10.0. Therefore, the optimal conditions for the ic-ELISA were an ionic strength of 290 mM NaCl and a pH of 7.0. In addition, we also evaluated the tolerability of mAb 10F8

to organic solvents (methanol and acetonitrile), and the results were shown in Fig. 1C, D, revealing that when the concentration of methanol reached 10% or the concentration of acetonitrile exceeded 5%, the OD_{max}/IC_{50} ratio fell significantly. In summary, the mAb 10F8 was not well tolerated in the organic solvents; therefore, pretreating the sample with an organic solvent may affect the sensitivity and accuracy of the immunoassay.

Under optimized immunoassay conditions, the sensitivity of ic-ELISA was assessed using a calibration curve constructed for AFM1 in PBS (Fig. 1E). The IC_{50} and analytical range (IC_{20} – IC_{80}) of ic-ELISA for AFM1 detection were 31.8 pg/mL and 8–129 pg/mL, respectively. There is no doubt that ic-ELISA with an ability to perform sub-ppt level detections lays the basis for further designing highly sensitive fluorescent immunoassays.

Besides, the specificity of mAb 10F8 was demonstrated by determining CRs against other mycotoxins (Fig. 1F), including AFM2, AFB1, AFB2, AFG1, AFG2, DON, ZEN, and OTA. The results indicated that the mAb 10F8 shows high specificity toward AFM1.

Working principle and performance of the automated and fluorescent immunoassay system

Figure 2 illustrates the working principle of the automated and fluorescent immunoassay system for highly sensitive AFM1 screening. As mentioned in the experimental section, all reagents needed for the immunoassay

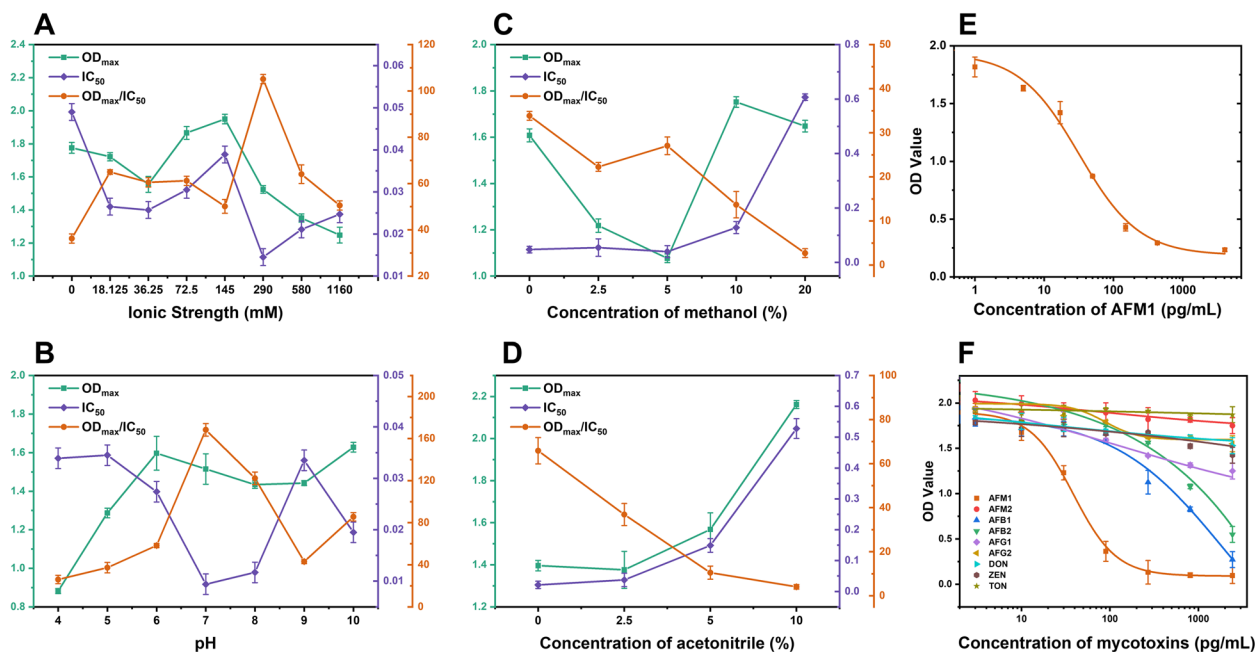


Fig. 1 Optimization of the physicochemical parameters on the ic-ELISA and the calibration curves assessed by the ic-ELISA. The effect of (A) ionic strength, (B) pH value, (C) methanol on the ic-ELISA. (D) acetonitrile on the ic-ELISA. (E) The calibration curve of ic-ELISA for AFM1 based on mAb 10F8. (F) Cross-reaction of AFM1 with various mycotoxin candidates based on mAb 10F8

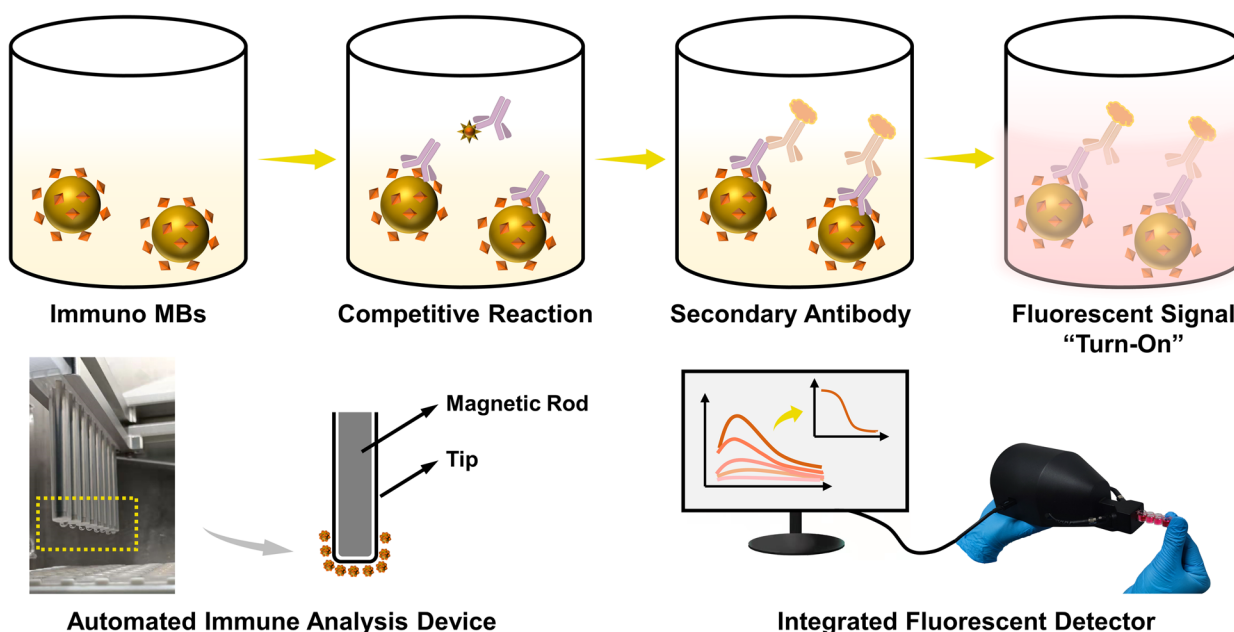


Fig. 2 Schematic illustration of the automated and fluorescent immunoassay system

were preloaded into a 96-well detachable ordinary microplate. First, mAb 10F8, immuno MBs, and various concentrations of AFM1 were introduced into column No. 2 simultaneously, and then immuno MBs and AFM1 competitively bound mAb 10F8. Due to the competitive nature of this method, increasing the concentration of AFM1 resulted in intense competition; as a result, fewer primary and secondary antibodies were bound to immuno MBs. Thus, by measuring the enzyme-catalyzed “turn-on” fluorescent signal (non-fluorescent amplex red reacts with H₂O₂ under HRP catalysis to produce red fluorescence at 582 nm resorcinol), we can precisely quantify the concentration of AFM1 in raw milk samples.

Because the fluorescent signal had an impact on the final quantification, the accuracy and stability of the self-designed integrated fluorescent detector were evaluated through comparisons with a commercial spectrofluorometer. Three solutions with different secondary antibody concentrations (0 to 20 ng/mL) and fluorescent substrates were prepared, and UV–Vis spectroscopy across a range of 500 to 700 nm was used to record the spectrum of the enzyme-catalyzed “turn-on” fluorescent signal. Distinctive emission peaks were evident at 582 nm (Fig. 3). Figure 3A (commercial spectrofluorometer) and Fig. 3B (integrated fluorescent detector) indicate that increasing the secondary antibody concentration led to an intensive enzyme-catalyzed reaction, and then, the high fluorescent signal was generated and measured.

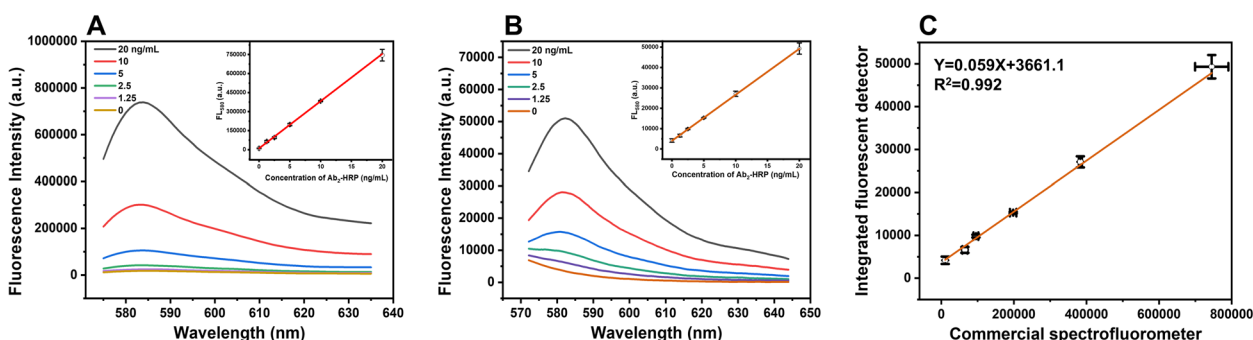


Fig. 3 Comparison of the integrated fluorescent detector and commercial spectrofluorometer. (A) Fluorescent intensity of the commercial spectrofluorometer used to measure the substrate. (B) Fluorescent intensity of the integrated fluorescent detector for measuring the substrate. (C) Correlation analysis between the fluorescent signal intensities of integrated fluorescent detector and commercial spectrofluorometer

More importantly, the fluorescence intensity recorded from the two above mentioned devices exhibited an excellent linear response, with a strong correlation value of $R^2=0.992$ (Fig. 3C). Therefore, the significant correlation between the two methods indicated that the integrated fluorescent detector can be utilized for fluorescent signal quantification.

Detection performance of the automated and fluorescent immunoassay system

We employed an automated and fluorescent immunoassay system to develop an indirect competitive immunoassay platform. In this study, the whole detection process, including the immune reaction and signal generation performed by the automated immunoassay system, was described in our previous work [34, 35]. After that, the “turn-on” fluorescent signal was quantified by the integrated fluorescent detector. To investigate the detection performance of the automated and fluorescent immunoassay system, we measured fluorescence spectra at various concentrations of AFM1 (0, 0.1, 0.8, 4.6, 27.8, 166.7, 1000, and 6000 pg/mL in PBS). Figure 4A shows the fluorescence spectra obtained from different AFM1 concentrations, ranging from 0 to 6000 pg/mL. It was observed that when AFM1 was gradually increased, more primary/secondary antibodies were inhibited, resulting in a decreased “turn-on” fluorescent intensity. We plotted the AFM1 concentration against the FL-FL_{ctrl} value (at 582 nm) to establish a four-parameter logistic curve. As shown in Fig. 4B, a standard curve (orange curve) was established by using the automated and fluorescent immunoassay system with a working range from 8 to 129 pg/mL (IC_{20} – IC_{80}). More satisfying, the IC_{50} of the automated and fluorescent immunoassay system was as low as 8.3 pg/mL. There is no doubt that the sensitivity

of the automated and fluorescent immunoassay system improved approximately fourfold when compared to that of traditional ic-ELISA (Fig. 4B purple curve). We attribute this high sensitivity to the following two key elements: (I) immuno MBs serve as an immune reaction carrier, and a semi-homogeneous reaction system was constructed to improve the efficiency of antigen and antibody recognition in immune reactions. (II) The strategy of enzyme-catalyzed “turn-on” enabled the amplification of fluorescent signals, background-free detection, and an excellent signal-to-noise ratio. Moreover, we automatize the whole immunoassay process using an automated immune analysis device and quantified the results using an integrated fluorescent detector. On the one hand, due to the use of automated and fluorescent immunoassay system, it is no longer necessary for operators to perform tedious manual operations. On the other hand, the low-cost and highly integrated fluorescent detector also provides a new idea for high-sensitivity detection targets in food items.

Application of the automated and fluorescent immunoassay system for AFM1 detection in raw milk samples

The feasibility of the automated and fluorescent immunoassay system was demonstrated by using actual raw milk samples. Different AFM1 concentrations were spiked into raw milk samples for analysis. After all reagents were preloaded into columns No. 1 to 10, the raw milk samples were injected into column No. 2 without any pretreatment. The automated and fluorescent immunoassay system worked automatically according to the set control program, and the total time consumption was ~37 min. In the recovery experiment, we spiked

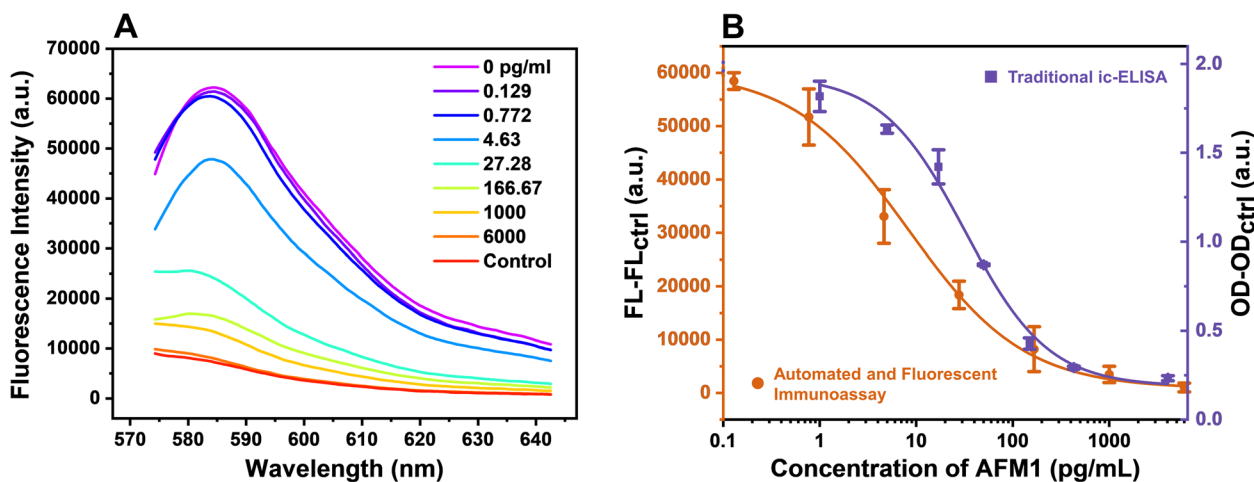


Fig. 4 Detection performance of the automated and fluorescent immunoassay system. (A) fluorescent spectra for different AFM1 concentrations (control: the solution including primary antibodies but no AFM1 or secondary antibodies). (B) The calibration curve of the automated and fluorescent immunoassay system and ic-ELISA for AFM1 based on mAb 10F8

samples at low, medium, and high concentrations. We used 0.2×, 1×, and 4× maximum concentrations (set in milk by the European Commission) as the low, medium, and high concentrations, respectively. The results of the recovery tests are listed in Table 1 and ranged from 79.0% to 104.6%. The assay reproducibility was satisfactory, with CVs under 15.2%. In our recovery experiments, we used raw milk, which has a more complicated food matrix than that of other types of milk, such as skim milk or whole milk. Gratifyingly, the results demonstrated the accuracy, practicality, and feasibility of the automated and fluorescent immunoassay system for the detection of AFM1 in raw milk samples. We attributed the excellent performance of the automated and fluorescent immunoassay system to the following reasons: immuno MBs serve as an immune reaction carrier in this system. All immunoassay steps were carried out in the automated immune analysis device. The washing effect of using this device could be significantly improved due to the homogeneous reaction system and the high specific surface area of the immuno MBs. Therefore, the removal effect of nonspecific substances in the complex matrix is better than that of traditional 96-well methods.

To increase the value of LOD in practical applications, the sensitivity of the automated and fluorescent immunoassay system was evaluated by using 20 blank raw milk samples. Satisfyingly, the LOD of the automated and fluorescent immunoassay system was 4.7 pg/mL, which is approximately 100-fold lower than the maximum limits set by China (500 pg/mL) and the United States (500 pg/mL) and 10-fold lower than the maximum limits set by the European Commission (50 pg/mL) for AFM1 in milk. We also compared our approach with various previously

Table 1 Recoveries and CV values for AFM1 in raw milk by the automated and fluorescent immunoassay system ($n=3$)

Spiked (pg/mL)	Tested (pg/mL)	Recoveries (%)	CVs (%)
10	7.9±0.2	79.0	8.9
50	52.3±1.3	104.6	13.6
200	165.4±13.5	82.7	15.2

published immunoassays for AFM1 detection and summarized the results in Table 2. More satisfying, the LOD of the automated and fluorescent immunoassay system was lower than those of the majority of the previously reported strategies. The reason for the high sensitivity lies in the strategy of using an enzyme-catalyzed fluorescent “turn-on” signal, which could provide a high signal-to-noise ratio. This serves as the foundation for ppt level detections of AFM1 by the integrated fluorescent detector.

To investigate the selectivity of the automated and fluorescent immunoassay system for AFM1 detection, several potential mycotoxins (AFM2, AFB1, AFB2, AFG1, AFG2, DON, ZEN, and OTA) were spiked into raw milk samples at a 20-fold concentration versus AFM1 (0.5 ng/mL) under the optimized conditions, and the fluorescent spectra of those mycotoxins are shown in Fig. 5A. As indicated in Fig. 5B, AFM1 exhibited negligible signals, whereas other mycotoxins (AFB1, AFM2, AFB2, AFG1, AFG2, DON, ZEN, and OTA) displayed strong fluorescent signals. These results demonstrated that the automated and fluorescent immunoassay system is highly selective for AFM1 analysis. Thus, the automated and fluorescent immunoassay system is extremely favorable and more suitable for AFM1 trace analysis in a complicated food matrix. In addition, the automated and fluorescent immunoassay system can be used to greatly simplify the assay procedure, as the system not only minimizes tedious manual operations but also reduces the risk of exposure to hazardous detection targets.

Conclusion

In this study, an automated and fluorescent immunoassay system was constructed for screening typical carcinogen, AFM1, in raw milk, and this system is advantageous in that no manual operation is necessary and highly sensitive quantification is achieved. First, we employed the immuno MBs as an immune reaction carrier, combined with the automated immunoassay system, to automate the whole immunoassay process. Then, the integrated fluorescent detector was self-designed, and this detector

Table 2 An overview of recent immunoassays for the detection of AFM1 in milk

Strategy	IC ₅₀ or Cut-off value (pg/mL)	Detection range (pg/mL)	LOD (pg/mL)	Reference
Indirect competitive enzyme-linked immunosorbent assay	IC ₅₀ : 620	320–500	40	[36]
Polystyrene microsphere-mediated optical sensing strategy	-	5–100,000	3.2	[37]
Gold nanoparticles modified electrode with Fe ³⁺ as a probe	-	1.6×10 ⁻¹⁵ –2500	1.6×10 ⁻¹⁵	[38]
Colorimetric Aptasensor	-	500–500,000	500	[39]
Mach–Zehnder Interferometric Immunosensor	-	100–2000	5	[40]
Automated and fluorescent immunoassay system	IC₅₀: 8.3	8–129	4.7	This work

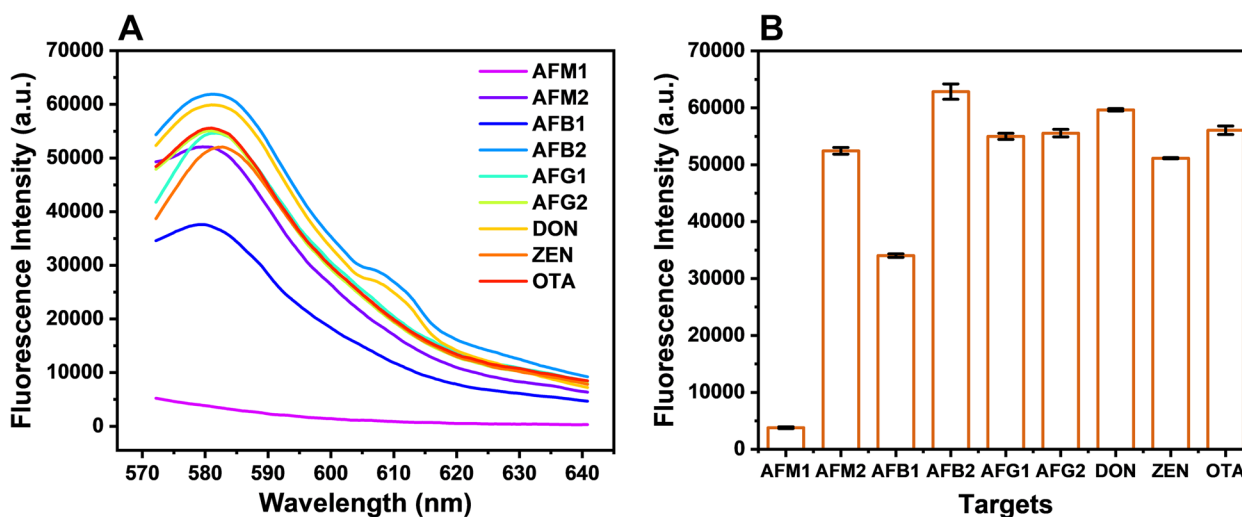


Fig. 5 The specificity of the automated and fluorescent immunoassay system was assessed by testing various mycotoxin candidates. **(A)** Fluorescent spectra for AFM1 and various mycotoxin candidates. **(B)** Fluorescent intensity for AFM1 and various mycotoxin candidates. AFM1 exhibited negligible signals in the immunoassay when tested at 0.5 ng/mL, whereas other mycotoxins displayed strong fluorescent signals at 10 ng/mL

can quantify the enzyme-catalyzed “turn-on” fluorescent signal after immunoassay with a high sensitivity. Compared with a commercial spectrofluorometer, the integrated fluorescent detector has several advantages including its small size (17*9*8 cm) and low cost (< 1900 USD), and the cost for one sample is ~1.12 USD (support information). It is highly suitable for performing on-site screening of AFM1 in milk. We comprehensively examined the performance of the automated and fluorescent immunoassay systems. The LOD for AFM1 in raw milk samples was as low as 4.7 pg/mL. The screening sensitivity with the ppt level is approximately 10- to 100-fold lower than the maximum limits set by China, the United States, and the European Commission for AFM1 in milk. In addition, the recovery experiment was carried out in complicated raw milk samples, and the results further demonstrated the advantages of the system in actual sample screening. In summary, the automated and fluorescent immunoassay system presented in this study has several advantages including a convenient operation, highly sensitive quantification, and low-cost. This study provides a new paradigm for the screening of trace typical carcinogens in milk.

Materials and methods

Materials and apparatus

AFM1, AFB1, aflatoxin M2 (AFM2), aflatoxin B2 (AFB2), aflatoxin G1 (AFG1), aflatoxin G2 (AFG2), deoxynivalenol (DON), zearalenone (ZEN), ochratoxin (OTA), key-hole limpet hemocyanin (KLH), bovine serum albumin (BSA), poly(ethylene glycol) (PEG) 1500, hypoxanthine

aminopterin thymidine (HAT), and red blood cell lysis buffer were purchased from Sigma–Aldrich (MO, USA). Freund’s complete adjuvant (FCA), Freund’s incomplete adjuvant (FIA), DMEM cell culture medium, and fetal calf serum were obtained from Gibco Life Technologies (NY, USA). Horseradish peroxidase-labeled goat anti-mouse IgG (gtAm-HRP) was purchased from Jackson ImmunoResearch (PA, USA). Fetal bovine serum (FBS), a mouse mAb isotyping kit, and streptavidin-coated magnetic beads Dynabeads™ MyOne™ Streptavidin T1 were purchased from Thermo Fisher Scientific (MA, USA). Amplex red was obtained from Beyotime (Shanghai, China). 1-[3-(Dimethylamino) propyl]-3-ethyl carbodi-imide hydrochloride (EDC HCl) and N-hydroxysuccinimide (NHS) were obtained from Aladdin Chemistry Co. Ltd. (Shanghai, China).

96-well detachable ordinary microplates were purchased from Costar (MA, USA). Deionized (DI) water was produced by a Milli-Q water purification system (MA, USA). The ELISA plate reader was acquired from PerkinElmer (MA, USA). An FS-5 spectrofluorometer was purchased from Edinburgh Instruments (EI, UK). The automated immune analysis device and optical fiber-based fluorescent detector were constructed in our laboratory.

Eight-week-old female BALB/c mice were obtained from Vital River Laboratory Animal Technology Co. Ltd. (Beijing, China), and all the animal experimental procedures were approved by the Animal Ethics Committee of China Agricultural University (Issue No:

AW32602202-2–4) and strictly conducted according to Chinese laws and guidelines.

AFM1 hapten synthesis

Hapten AFM1-CMO was prepared by inserting a carboxyl into the cyclopentenone moiety of AFM1 [15, 16] (Fig. S4). Briefly, 2.0 mg of carboxymethoxylamine hemihydrochloride (CMO) was added to 1.0 mg/mL AFM1 in pyridine, and then the mixture was stirred at room temperature for 48 h. Afterward, the reaction mixture was spotted onto silica thin-layer chromatography (TLC) plates and developed in chloroform:methanol (9:1) with 1.5% acetic acid. Subsequently, the reaction product was observed under 365 nm UV light. When the reaction was finished, the reaction mixture was immediately placed under N₂ gas and evaporated to dryness to obtain AFM1-CMO.

Preparation of immunogen and coating antigen

The hapten AFM1-CMO was conjugated to the carrier proteins KLH and BSA through the active-ester method to obtain the immunogen (AFM1-KLH) and coating antigen (AFM1-BSA). Briefly, 2.0 mg of AFM1-CMO was dissolved in 2.0 mL of dimethylformamide (DMF), followed by the addition of 1.8 mg of NHS and 3.0 mg of EDC. After stirring at room temperature for 4 h, 1.5 mL of the mixture was added dropwise to a KLH solution (25 mg KLH dissolved in 9.0 mL of 0.05 M carbonate bicarbonate buffer). Another 1.5 mL of the mixture was added slowly dropwise to a BSA solution (8.3 mg BSA dissolved in 3.0 mL of 0.05 M carbonate bicarbonate buffer) with continuous stirring. The two mixtures were further stirred for 14 h at room temperature; then, the conjugates were purified by dialysis against phosphate-buffered saline (PBS) for 3 days and stored at 20 °C.

Preparation of the monoclonal antibody

Eight female BALB/c mice were immunized with AFM1-KLH to produce monoclonal antibodies (mAb) against AFM1. For the first immunization, the mice were injected with 200 µL of a mixture (v/v, 1:1) of immunogen (AFM1-KLH) and FCA. After three weeks, two subsequent immunizations were carried out at three-week intervals by using a mixture of immunogen and FIA at the same dosage. One week after the last booster injection, the titer and selectivity of the antiserum in each mouse were tested. The mice that exhibited a high antibody titer and inhibition rate were boosted intraperitoneally with 150 µg immunogen in 500 µL before three days for cell fusion.

Spleen cells from the immunized mice were collected and washed with DMEM and then fused with SP2/0 cells at a ratio of 5:1 (the total number of cells was 1×10^8)

using 800 µL of prewarmed PEG1500. Afterward, the fused cells were cultured in 20 96-well plates containing 20% HAT medium. One week later, the supernatant was tested, and the positive hybridomas were screened using ic-ELISA and subcloned twice by the limiting dilution method. After that, the monoclonal hybridoma cells with the highest affinity and inhibition were selected for the large-scale production of ascites. The isotype class and subclass of the produced mAbs were identified by using a mouse mAb isotyping kit, and the mAbs were purified from ascites using a protein A column and then stored at -20 °C for further use.

Traditional ic-ELISA procedures were conducted as follows: each well of the microplates was coated with 100 µL of diluted AFM1-BSA in coating buffer (0.05 M carbonate bicarbonate, pH 9.6) and then incubated at 4 °C for 16 h. The plates were washed once with PBST (PBS containing 0.05% Tween 20 (v/v), pH 7.4) and then blocked with 150 µL of blocking buffer (3% BSA in PBS, pH 7.4), which was incubated at 37 °C for 1 h to avoid nonspecific binding. After the blocking buffer was discarded, 50 µL of serially diluted AFM1 and 50 µL of anti-AFM1 mAb were added to a 96-well plate and incubated at 37 °C for 30 min for the competitive reaction. After three washes, 100 µL of gtAm-HRP (diluted 1:5000 in PBS, pH 7.4) was added to each well and incubated at 37 °C for another 30 min. The plates were washed four times, 100 µL of 3,3',5,5'-tetramethylbenzidine (TMB) substrate was added and incubated for 15 min at room temperature, and the reaction was halted by adding 50 µL per well of stop solution (2.0 M H₂SO₄). Afterward, the OD value of the wells was measured at 450 nm by an ELISA plate reader.

Preparation of immuno magnetic beads

The biotinylated coating antigen was first produced; briefly, 70 µL of activated biotin ester (1 mg/mL) and 500 µL of AFM1-BSA (1.668 mg/mL) were mixed in a 1.5 mL tube and reacted at 25 °C for 4 h in the dark. The 45 µL of biotinylated AFM1-BSA (0.7 mg/mL) was obtained by ultrafiltration with a 5 kD membrane, which was performed three times. After that, the diluted 3 mL of the biotinylated AFM1-BSA solution (0.15 µg/mL in PBS) was added to 80 µL of the streptavidin-coated MB solution (10 mg/mL in PBS), and the mixed solution was placed in a micro oscillator to react at room temperature for 15 min. Following this, biotinylated AFM1-BSA was attached to the surface of streptavidin-coated magnetic beads due to the high affinity of biotin to streptavidin. Finally, the coating antigen-functionalized magnetic beads (immuno MBs) were washed twice with 2 mL 0.1% PBST and blocked with 3% BSA in PBS at 37 °C for 15 min before being redissolved to 400 µg/mL and kept at 4 °C.

Principle of the automated and fluorescent immunoassay system

The principle of the automated immunoassay system was performed based on previous studies in our laboratory, with slight modifications [34, 35] (Fig. 2). In this study, we utilized 96-well detachable ordinary microplates. All reagents were preloaded in columns No. 1 to 10: 150 μ L of washing buffer (0.1% PBST, pH 7.4) per column was added to columns No. 1, 3, 4, 5, 7, 8, and 9; 20 μ L of immuno MBs and 40 μ L of mAb 10F8 (with the best affinity to AFM1) solution (0.11 μ g/mL) were added to column No. 2; 100 μ L of gtAm-HRP (200 ng/mL) was added to column No. 6; and 100 μ L of fluorescent substrate (a mixture of 100 μ M amplex red and 20 μ M hydrogen peroxide) was added to column No. 10 (Table S2). For the detection of AFM1 in raw milk samples (All milk samples were raw milk, that is, milk samples were collected from farms without any treatment), we only needed to inject the samples into column No. 2, and the automated immunoassay system was performed in the order of No. 2–1–3–4–6–5–7–8–9–10, sequentially. The incubation for the competition reaction and secondary antibody binding was set to 30 min at 37 °C, the generation of enzyme-catalyzed “turn-on” signals was set to 15 min at room temperature, and all the washing steps were set to 2 min at room temperature.

After the “turn-on” fluorescent signal was generated, the 8-well trip of column No. 10 was removed from the 96-well detachable ordinary microplates, and the fluorescent intensity in each well was measured by an integrated fluorescent detector that was optical fiber-based and self-designed for quantification (Fig. 2). The integrated fluorescent detector was composed of a miniature spectrometer (STS-VIS, Ocean Optics, 1580 USD), an excitation light source (BIM-6215, 565 nm LED, Brolight Technology, 260 USD), two optical fibers (HFBR4511, plastic optical fiber, Avago Technologies, 18 USD), and a housing (Resin 3D-printing, Sogaworks Technologies, 25 USD). A schematic diagram is shown in Fig. S5.

Analysis of trace mounts of AFM1 in raw milk samples

The applicability of the automated and fluorescent immunoassay to milk samples was evaluated by analyzing commercial raw milk, and the analysis confirmed that there was no AFM1 contamination. In the recovery experiments, we spiked samples with various doses of AFM1 (10, 50, and 200 pg/mL). Notably, the raw milk sample was directly injected into the automated and fluorescent immunoassay system without any pretreatment. The fluorescent signals were analyzed using OriginPro 9.1 (OriginLab, MA, United States) utilizing a four-parameter logistic regression function to obtain a standard curve. The limit of detection (LOD) was determined as

the mean value of 20 blank samples plus three times the standard deviation [41]. The specificity of the proposed immunoassay was investigated by comparing AFM1 with other potential mycotoxin contaminants in raw milk, such as AFM2, AFB1, AFB2, AFG1, AFG2, DON, ZEN, and OTA. The cross-reactivity (CR) was calculated by measuring the fluorescent signal of each of these targets.

Supplementary Information

The online version contains supplementary material available at <https://doi.org/10.1186/s44280-024-00040-4>.

Additional file 1: Fig. S1. MALDI-TOLF-MS result of AFM1-BSA. **Fig. S2.** The isotypes determination of four mAbs. **Fig. S3.** Combination of three coating antigens and four mAbs in the ic-ELISA. (A) ODmax (means the OD value of negative control) of three coating antigens and four mAbs in the ic-ELISA. (B) IC50 of three coating antigens and four mAbs in the ic-ELISA. (C) ODmax/IC50 of three coating antigens and four mAbs in the ic-ELISA. **Fig. S4.** Chemical structure and synthesis route used in the study. **Fig. S5.** Schematic diagram of the integrated fluorescent detector. (A) Miniature spectrometer. (B) Excitation light source. (C) Two optical fibers. (D) 3D-printed housing. **Table S1.** Combination of three coating antigens and four mAbs in the ic-ELISA. **Table S2.** Microplate column code and corresponding reagent added.

Acknowledgements

We sincerely thank all the members that provided the raw milk samples.

Authors' contributions

W.Y. designed the experiments; J.K. wrote the manuscript; J.K., L.D., W.W. and Y.Z. performed the experiments; P.L., X.W., G.M.M. and K.W. analysed the data; S.Z., Y.P. and W.Y. provided discussion and revised the manuscript. All authors read and approved the final manuscript.

Funding

This project has received funding from the National Natural Science Foundation of China under Grant 31902320. The Key R&D Program of Ningxia Hui Autonomous Region (2021BBF02036).

Availability of data and materials

The datasets used and/or analysed during the current study are available from the corresponding author on reasonable request.

Declarations

Ethics approval and consent to participate

All the animal experimental procedures were approved by the Animal Ethics Committee of China Agricultural University (Issue No: AW32602202–2–4) and strictly conducted by Chinese laws and guidelines.

Competing interests

The authors declare that they have no competing interests.

Received: 1 July 2023 Revised: 21 January 2024 Accepted: 18 February 2024

References

1. Wood GE. Mycotoxins in foods and feeds in the United States. *J Anim Sci.* 1992;70:3941–9. <https://doi.org/10.2527/1992.70123941x>.
2. Muaz K, Riaz M, Akhtar S, Ali SW, Nadeem H, Park S, et al. Aflatoxin M1 in milk and dairy products: global occurrence and potential

- decontamination strategies. *Toxin Reviews*. 2022;41:588–605. <https://doi.org/10.1080/15569543.2021.1873387>.
- Turna NS, Wu F. Aflatoxin M1 in milk: a global occurrence, intake, & exposure assessment. *Trends Food Sci Technol*. 2021;110:183–92. <https://doi.org/10.1016/j.tifs.2021.01.093>.
 - Salari N, Kazemini M, Vaisi-Raygani A, Jalali R, Mohammadi M. Aflatoxin M1 in milk worldwide from 1988 to 2020: a systematic review and meta-analysis. *J Food Qual Hazards Control*. 2020;2020:1–14. <https://doi.org/10.1155/2020/8862738>.
 - IARC working group on the evaluation of carcinogenic risks to humans. Some traditional herbal medicines, some mycotoxins, naphthalene, and styrene. *IARC Monogr Eval Carcinog Risks Hum*. 2002;82:1–556.
 - National Health and Family Planning Commission of the People's Republic of China, China Food and Drug Administration. National standard for food safety - limits of mycotoxins in food. No. GB 2761–2017. 2017.
 - Peng D, Yang B, Pan Y, Wang Y, Chen D, Liu Z, et al. Development and validation of a sensitive monoclonal antibody-based indirect competitive enzyme-linked immunosorbent assay for the determination of the aflatoxin m1 levels in milk. *Toxicol*. 2016;113:18–24. <https://doi.org/10.1016/j.toxicol.2016.02.006>.
 - Food and Drug Administration (FDA). SEC 527.400 Whole Milk, Low fat Milk, Skim Milk - Aflatoxin M1. CPG 7106.10. 2005.
 - Yao H, Hruska Z, Di Mavungu JD. Developments in detection and determination of aflatoxins. *World Mycotoxin J*. 2015;8:181–91. <https://doi.org/10.3920/wmj.2014.1797>.
 - The Commission of European Communities. Regulation (EU) No. 1881/2006 of 19 December 2006 - Setting maximum levels for certain contaminants in foodstuffs. *Off J EU*. 2006;L364:5–24.
 - Busman M, Bobell JR, Maragos CM. Determination of the aflatoxin m1 from milk by direct analysis in real time - mass spectrometry (dart-ms). *Food Control*. 2015;2015(47):592–8. <https://doi.org/10.1016/j.foodcont.2014.08.003>.
 - Cavaliere C, Foglia P, Pastorini E, Samperi R, Lagana A. Liquid chromatography/tandem mass spectrometric confirmatory method for determining aflatoxin m1 in cow milk - comparison between electrospray and atmospheric pressure photoionization sources. *J Chromatogr A*. 2006;1101:69–78. <https://doi.org/10.1016/j.chroma.2005.09.060>.
 - Solfrizzo M, Gambacorta L, Lattanzio VMT, Powers S, Visconti A. Simultaneous LC-MS/MS determination of aflatoxin M₁, ochratoxin A, deoxynivalenol, de-epoxydeoxynivalenol, alpha and beta-zearalenols and fumonisin B₁ in urine as a multi-biomarker method to assess exposure to mycotoxins. *Anal Bioanal Chem*. 2011;401:2831–41. <https://doi.org/10.1007/s00216-011-5354-z>.
 - Chavarria G, Granados-Chinchilla F, Alfaro-Cascante M, Molina A. Detection of aflatoxin m1 in milk, cheese and sour cream samples from costa rica using enzyme-assisted extraction and HPLC. *Food Addit Contam Part B Surveill*. 2015;8:128–35. <https://doi.org/10.1080/19393210.2015.1015176>.
 - Zhang XY, Song MR, Yu XZ, Wang ZH, Ke YB, Jiang HY, et al. Development of a new broad-specific monoclonal antibody with uniform affinity for aflatoxins and magnetic beads-based enzymatic immunoassay. *Food Control*. 2017;79:309–16. <https://doi.org/10.1016/j.foodcont.2017.02.049>.
 - Zhang X, Wen K, Wang Z, Jiang H, Beier RC, Shen J. An Ultra-sensitive monoclonal antibody-based fluorescent microsphere immunochromatographic test strip assay for detecting aflatoxin M₁ in milk. *Food Control*. 2016;60:588–95. <https://doi.org/10.1016/j.foodcont.2015.08.040>.
 - Dou LN, Bai YC, Liu MG, Shao SB, Yang HJ, Yu XZ, et al. "Three-To-One" multi-functional nanocomposite-based lateral flow immunoassay for label-free and dual-readout detection of pathogenic bacteria. *Biosens Bioelectron*. 2022;204:114093. <https://doi.org/10.1016/j.bios.2022.114093>.
 - Wang L, Lin JH. Recent advances on magnetic nanobead based biosensors: from separation to detection. *TrAC Trends Anal Chem*. 2022;128:115915. <https://doi.org/10.1016/j.trac.2020.115915>.
 - Blaskova A, Kveton F, Lorencova L, Blixt O, Vikartovska A, Kasak P, et al. Amplified suspension magnetic bead-based assay for sensitive detection of anti-glycan antibodies as potential cancer biomarkers. *Anal Chim Acta*. 2022;1195:339444. <https://doi.org/10.1016/j.aca.2022.339444>.
 - Onishi T, Mihara K, Matsuda S, Sakamoto S, Kuwahata A, Sekino M, et al. Application of magnetic nanoparticles for rapid detection and in situ diagnosis in clinical oncology. *Cancers*. 2022;14:364. <https://doi.org/10.3390/cancers14020364>.
 - Dong YZ, Chen R, Wu L, Wang XH, Jiang F, Fan ZY, et al. Magnetic relaxation switching biosensor via polydopamine nanoparticle mediated click chemistry for detection of chlorpyrifos. *Biosens Bioelectron*. 2022;207:114127. <https://doi.org/10.1016/j.bios.2022.114127>.
 - Shen Y, Jia F, Liang A, He Y, Peng Y, Dai H, et al. Monovalent antigen-induced aggregation (maa) biosensors using immunomagnetic beads in both sample separation and signal generation for label-free detection of enrofloxacin. *ACS Appl Mater Interfaces*. 2022;14:8816–23. <https://doi.org/10.1021/acsmami.1c23398>.
 - Dong BL, Li HF, Sun JF, Li Y, Mari GM, Yu XZ, et al. Magnetic assisted fluorescence immunoassay for sensitive chloramphenicol detection using carbon dots@CaCO₃ nanocomposites. *J Hazard Mater*. 2021;402:123940. <https://doi.org/10.1016/j.hazmat.2020.123942>.
 - Dong BL, Li HF, Mari GM, Yu XZ, Yu WB, Wen K, et al. Fluorescence immunoassay based on the inner-filter effect of carbon dots for highly sensitive amantadine detection in foodstuffs. *Food Chem*. 2019;2019(294):347–54. <https://doi.org/10.1016/j.foodchem.2019.05.082>.
 - Li HF, Dong BL, Dou LN, Yu WB, Yu XZ, Wen K, et al. Fluorescent lateral flow immunoassay for highly sensitive detection of eight anticoagulant rodenticides based on cadmium-free quantum dot-encapsulated nanospheres. *Sens Actuator B-Chemical*. 2020;324:128771. <https://doi.org/10.1016/j.snb.2020.128771>.
 - Yu WB, Li Y, Xie B, Ma MF, Chen CC, Li CL, et al. An aggregation-induced emission-based indirect competitive immunoassay for fluorescence "turn-on" detection of drug residues in foodstuffs. *Front Chem*. 2019;7:228. <https://doi.org/10.3389/fchem.2019.00228>.
 - Yu WB, Jiang CX, Xie B, Wang SY, Yu XZ, Wen K, et al. Ratiometric fluorescent sensing system for drug residue analysis: highly sensitive immunosensor using dual-emission quantum dots hybrid and compact smartphone based-device. *Anal Chim Acta*. 2020;2020(1102):91–8. <https://doi.org/10.1016/j.aca.2019.12.037>.
 - Dong BL, Li HF, Sun JF, Mari GM, Yu XZ, Ke YB, et al. Development of a fluorescence immunoassay for highly sensitive detection of amantadine using the nanoassembly of carbon dots and MnO₂ nanosheets as the signal probe. *Sens Actuator B-Chemical*. 2019;286:214–21. <https://doi.org/10.1016/j.snb.2019.01.100>.
 - Cheng Y, Wang HL, Zhuo YX, Song D, Li CS, Zhu AN, et al. Reusable smartphone-facilitated mobile fluorescence biosensor for rapid and sensitive on-site quantitative detection of trace pollutants. *Biosens Bioelectron*. 2022;199:11386. <https://doi.org/10.1016/j.bios.2021.113863>.
 - Long F, Li W, Song D, Han X, Zhou Y, Fang S, et al. Portable and automated fluorescence microarray biosensing platform for on-site parallel detection and early-warning of multiple pollutants. *Talanta*. 2020;210:1206–50. <https://doi.org/10.1016/j.talanta.2019.120650>.
 - Chen LB, Wen K, Chen FE, Trick AY, Liu HB, Shao SB, et al. Portable magnetofluidic device for point-of-need detection of african swine fever. *Anal Chem*. 2021;93:10940–6. <https://doi.org/10.1016/j.jaca.2021.339345>.
 - Zhao SQ, Chen XJ, Huang JW, Zhang XN, Sun JL, Yang L. Point-of-care testing of methylamphetamine with a portable optical fiber immunosensor. *Anal Chim Acta*. 2022;1192:339345. <https://doi.org/10.1016/j.aca.2021.339345>.
 - Nie RB, Huang JW, Xu XX, Yang L. Immunoassays using optical-fiber sensor with all-directional chemiluminescent collection. *Anal Chem*. 2020;92:6257–62. <https://doi.org/10.1021/acs.analchem.0c00882>.
 - Zhu JY, Dou LA, Shao SB, Kou JQ, Yu XZ, Wen K, et al. An automated and highly sensitive chemiluminescence immunoassay for diagnosing mushroom poisoning. *Front Chem*. 2021;9:813219. <https://doi.org/10.3389/fchem.2021.813219>.
 - Yu WB, Hu MF, Qi WZ, Dou LN, Pan YT, Bai YC, et al. From pretreatment to assay: a chemiluminescence- and optical fiber-based fully automated immunosensing (COFFAI) system. *Sens Actuator B-Chemical*. 2022;362(9):131820. <https://doi.org/10.1016/j.snb.2022.131820>.
 - Pei SC, Zhang YY, Eremin SA, Lee WJ. Detection of aflatoxin M1 in milk products from China by ELISA using monoclonal antibodies. *Food Control*. 2009;20(12):1080–5. <https://doi.org/10.1016/j.foodcont.2009.02.004>.
 - Zhou CY, Pan SX, Liu PY, Feng N, Lu P, Wang PL, et al. Polystyrene microsphere-mediated optical sensing strategy for ultrasensitive determination of aflatoxin M₁ in milk. *Talanta*. 2023;258. <https://doi.org/10.1016/j.talanta.2023.124357>.

38. Li XB, Zhang M, Mo HZ, Li HB, Xu D, Hu LB. The ultrasensitive detection of aflatoxin M₁ using gold nanoparticles modified electrode with Fe³⁺ as a probe. *Foods*. 2023;12(13):2521. <https://doi.org/10.3390/foods12132521>.
39. Wei XJ, Ma PF, Mahmood KI, Zhang Y, Wang ZP. Screening of a high-affinity aptamer for aflatoxin M₁ and development of its colorimetric aptasensor. *J Agric Food Chem*. 2023;71(19):7546–56. <https://doi.org/10.1021/acs.jafc.3c01586>.
40. Angelopoulou M, Kourti D, Misiakos K, Economou A, Petrou P, Kakabakos S. Mach-zehnder interferometric immunosensor for detection of aflatoxin M₁ in milk, chocolate milk, and yogurt. *Biosensors*. 2023;13(6):592. <https://doi.org/10.3390/bios13060592>.
41. Shahdeo D, Khan AA, Alanazi AM, Bajpai VK, Shukla S, Gandhi S. Molecular diagnostic of ochratoxin a with specific aptamers in corn and groundnut via fabrication of a microfluidic device. *Front Nutr*. 2022;9:851787. <https://doi.org/10.3389/fnut.2022.851787>.

Publisher's Note

Springer Nature remains neutral with regard to jurisdictional claims in published maps and institutional affiliations.